Title

Helicobacter pylori Uses the TlpB Receptor To Sense Sites of Gastric Injury.

Journal

Infection and Immunity, 87(9)

ISSN

0019-9567

Authors

Hanyu, Hikaru
Engevik, Kristen A
Matthis, Andrea L
et al.

Publication Date

2019-09-01

DOI

10.1128/iai.00202-19

Peer reviewed

AMERICAN SOCIETY FOR MICROBIOLOGY | Infection and Immunity®

CELLULAR MICROBIOLOGY:
PATHOGEN-HOST CELL MOLECULAR INTERACTIONS

Helicobacter pylori Uses the TlpB Receptor To Sense Sites of Gastric Injury

Hikaru Hanyu,[a] Kristen A. Engevik,[a] Andrea L. Matthis,[a] Karen M. Ottemann,[b] Marshall H. Montrose,[a] Eitaro Aihara[a]

[a]Department of Pharmacology and Systems Physiology, College of Medicine, University of Cincinnati, Cincinnati, Ohio, USA
[b]Department of Microbiology and Environmental Toxicology, University of California—Santa Cruz, Santa Cruz, California, USA

ABSTRACT *Helicobacter pylori* is a pathogen that chronically colonizes the stomachs of approximately half of the world's population and contributes to the development of gastric inflammation. We demonstrated previously *in vivo* that *H. pylori* uses motility to preferentially colonize injury sites in the mouse stomach. However, the chemoreceptor responsible for sensing gastric injury has not yet been identified. In this study, we utilized murine gastric organoids (gastroids) and mutant *H. pylori* strains to investigate the components necessary for *H. pylori* chemotaxis. High-intensity 730-nm light (two-photon photodamage) was used to cause single-cell damage in gastroids, and repair of the damage was monitored over time; complete repair occurred within ~10 min in uninfected gastroids. Wild-type *H. pylori* accumulated at the damage site after gastric damage induction. In contrast, mutants lacking motility (Δ*motB*) or chemotaxis (Δ*cheY*) did not accumulate at the injury site. Using mutants lacking individual chemoreceptors, we found that only TlpB was required for *H. pylori* accumulation, while TlpA, TlpC, and TlpD were dispensable. All strains that were able to accumulate at the damage site limited repair. When urea (an identified chemoattractant sensed by TlpB) was microinjected into the gastroid lumen, it prevented the accumulation of *H. pylori* at damage sites. Overall, our findings demonstrate that *H. pylori* colonizes and limits repair at damage sites via chemotactic motility that requires the TlpB chemoreceptor to sense signals generated by gastric epithelial cells.

KEYWORDS *Helicobacter pylori*, TlpB, chemotaxis, gastric organoids, injury, intravital microscopy, pathogenesis, photodamage, repair, stomach

Helicobacter pylori is a pathogen that colonizes the stomach and contributes to the development of gastric inflammation (1). *H. pylori* resides chronically in half of the world's population, in both developing and developed countries, although 90% of these cases are asymptomatic (2). Therefore, the trigger responsible for *H. pylori* pathogenesis remains unclear. We demonstrated previously *in vivo* that pathogenic *H. pylori* preferentially colonizes injury sites of the stomach using its chemotaxis system (3). However, it has yet to be elucidated which chemoattractants and respective *H. pylori* chemoreceptors are essential for this preferential colonization.

H. pylori uses a chemotaxis system to modulate its motility and rapidly establish colonization near the gastric epithelium (4). *H. pylori* senses chemoattractants or repellents by using four chemoreceptors: TlpA, TlpB, TlpC, and TlpD. *H. pylori* mutants lacking these chemoreceptors (Δ*tlpA*, Δ*tlpB*, Δ*tlpC*, or Δ*tlpD* mutants) are motile (5, 6) but are unable to sense their respective chemoattractants or repellents. Numerous signals are sensed by these chemoreceptors, including arginine by TlpA (7), urea and autoinducer 2 (AI-2) by TlpB (8, 9), lactate by TlpC (10), acid by TlpA, TlpB, and TlpD (11), and reactive oxygen species (ROS) and cellular energy by TlpD (6, 12). While several signals have been confirmed for specific *H. pylori* chemoreceptors, additional *H. pylori*

Citation Hanyu H, Engevik KA, Matthis AL, Ottemann KM, Montrose MH, Aihara E. 2019. *Helicobacter pylori* uses the TlpB receptor to sense sites of gastric injury. Infect Immun 87:e00202-19. https://doi.org/10.1128/IAI.00202-19.

Editor Vincent B. Young, University of Michigan—Ann Arbor

Address correspondence to Marshall H. Montrose, mhm@uc.edu, or Eitaro Aihara, aiharaeo@uc.edu.

Received 11 March 2019
Returned for modification 9 April 2019
Accepted 18 June 2019
Accepted manuscript posted online 1 July 2019
Published 21 August 2019

signals that have yet to be identified may be present in the gastric environment. Upon sensing gradients of signaling compounds, chemoreceptors activate signal transduction proteins in the Che family. CheY is the most downstream member of the Che proteins and interacts directly with the flagellar motor to control the direction of flagellar rotation. *H. pylori* mutants lacking CheY (Δ*cheY*) are motile but are unable to control the direction of flagellar rotation (13). The flagellar motor is controlled by proteins of the Mot family. *H. pylori* mutants lacking MotB (Δ*motB*) are nonmotile, since they retain only a nonfunctioning flagellar structure (14).

Currently, 3-dimensional primary culture of gastric epithelial cells (15, 16), called gastric organoids (gastroids), has been utilized as a model for *H. pylori* infection studies (17, 18). We have recently established gastroids as a restitution model with which to investigate actin dynamics (19). Restitution is the initial step during the repair process; it is characterized by cell migration and does not involve cell proliferation. During restitution, viable cells neighboring the injury site migrate to cover the denuded area while simultaneously exfoliating the dead cell into the lumen; this event is completed within ~10 min in response to two-photon-induced single-cell damage in gastroids (19, 20).

In this study, we utilize mouse-derived gastroids to explore the sensing of an injury site by *H. pylori* chemoreceptors. Using gastroids as a reductionist model, we are able to recapitulate gastric epithelial events during restitution and to observe the *H. pylori* chemotaxis response closely. Gastroids provide the opportunity to monitor the initial interactions of *H. pylori* with the gastric epithelium in the absence of other systemic elements, such as the immune system.

RESULTS

Wild-type *H. pylori* accumulates at the damage site during restitution. We first asked if *H. pylori* utilizes chemotaxis to colonize damage sites in the gastroid model, a mechanism similar to that observed previously in the mouse stomach *in vivo* (3). To address this question, gastroids were generated from isolated corpus tissue of human green fluorescent protein (GFP)-actin-expressing (HuGE) transgenic mice (19–21). *H. pylori* Sydney strain 1 (wild type [WT]) or fluorescent beads were microinjected into gastroids. Following injection, gastroids were injured using localized photodamage (PD), which induces cell death at the single-cell level. In agreement with previous findings (19), PD caused a loss of GFP-actin fluorescence within the damaged cell, as well as the migration of neighboring cells toward the site of damage. Finally, the damaged cell (nucleus stained by Hoechst 33342) was expelled into the gastroid lumen. These events were accompanied by actin redistribution, visualized as a localized increase in the level of GFP-actin fluorescence in the migrating cells.

After microinjection and PD, fluorescent beads remained distributed through the gastroid lumen and did not accumulate at the site of injury (Fig. 1A). We used fluorescence intensity ratios, comparing the damaged area of the gastroid to the gastroid lumen, as a measure of fluorescence accumulation at the damage site. We observed that fluorescent beads maintained an even distribution in the gastroids as long as 16 min following PD (Fig. 1B and D). In contrast, fluorescently labeled (CellTrace) WT *H. pylori* accumulated significantly at the damaged site (Fig. 1A, B, and D; see also Movie S1 in the supplemental material). To confirm these findings, we also monitored WT *H. pylori* genetically tagged with red fluorescent protein (RFP). In agreement with our findings using the CellTrace label, RFP-tagged WT *H. pylori* also accumulated at the damage site (see Movie S2), confirming that the accumulation of *H. pylori* is not affected by the surface label. WT *H. pylori* rapidly accumulated at the damage site, starting at 3 min after PD (Fig. 1B and D). The results suggest that the damaged gastric epithelium is sufficient to generate chemotactic signals without the other tissue cell types present *in vivo*.

Microinjection of fluorescent beads had no effect on PD-induced gastric restitution, where we observed a complete elimination of the damaged area, as seen in previous studies (19, 20). Based on measurement of the damaged area, WT *H. pylori* limited the

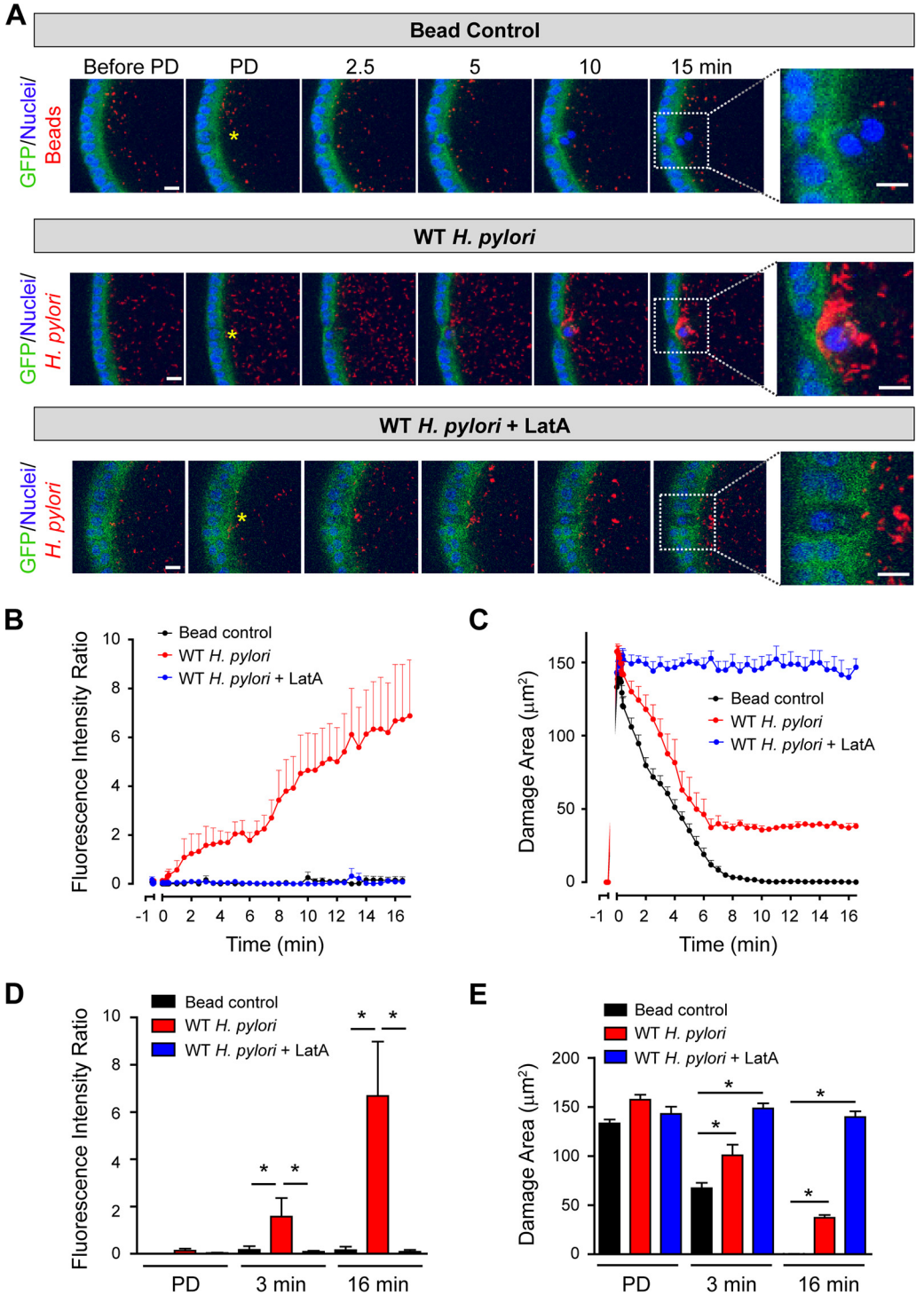

FIG 1 *H. pylori* accumulates at the damage site and delays restitution in gastroids. WT *H. pylori* was labeled with CellTrace Far Red fluorescent dye. Brucella broth (50 nl) containing 10^5 fluorescent beads or 10^6 WT *H. pylori* cells was microinjected into each gastroid. Latrunculin A (LatA) (1 μM) was added to the gastroid growth medium 1 h prior to *H. pylori* microinjection. Photodamage (PD) was induced at 0 min. (A) Representative time course. Confocal images show Hoechst 33342 (10 μg/ml)-stained nuclei (blue), GFP-actin (green), and the fluorescent bead control (red) or WT *H. pylori* (red) with or without Latrunculin A. Yellow asterisks indicate single-cell PD sites. Bars, 10 μm. (B and C) Time course of the fluorescence intensity ratio (B) or the damaged area (C) in gastroids microinjected with WT *H. pylori* alone (red), WT *H. pylori* in the presence of Latrunculin A (blue), or a bead control (black). The fluorescence intensity ratio is calculated as the raw fluorescence at the injury site divided by the raw fluorescence in the lumen. (D and E) Measurements of the fluorescence intensity ratio (D) and the damaged area in gastroids (E) during and following PD at 0 min, 3 min, and 16 min. Compiled results are means ± SEM for fluorescent beads ($n = 8$), WT *H. pylori* alone ($n = 5$), or WT *H. pylori* with Latrunculin A ($n = 5$). Asterisks indicate significance ($P < 0.05$) by one-way repeated-measures ANOVA with Bonferroni's multiple-comparison test.

restitution of the damage site relative to that with the fluorescent-bead control (Fig. 1C and E), a result also similar to previous findings *in vivo* (3). Interestingly, while *H. pylori* delayed repair, it did not affect actin redistribution (see Fig. S1 in the supplemental material). This suggests that short-term *H. pylori* infection has no immediate effect on actin dynamics, despite the ability to inhibit proper restitution in the same time interval.

To determine if the process of epithelial repair was necessary for *H. pylori* accumulation, we inhibited actin polymerization with Latrunculin A (LatA), a specific actin polymerization inhibitor. Actin polymerization is essential for initiating dead-cell exfoliation and cell migration during restitution in gastroids (19). We confirmed that Latrunculin A inhibited gastric restitution in a concentration-dependent manner (see Fig. S2 in the supplemental material) and observed that the concentrations tested did not grossly affect *H. pylori* motility or morphology (see Movie S3A, B, C, and D). In agreement with previous studies (19), we observed that preincubation of gastroids with 1 μM Latrunculin A completely inhibited gastric restitution (Fig. 1A, C, and E). We found that the accumulation of WT *H. pylori* at the damage site in gastroids was strongly inhibited by Latrunculin A (Fig. 1A, B, and D). This shows that *H. pylori* chemotaxis relies on a process that is disrupted by Latrunculin A, likely either an action of the migrating cells to generate the chemosensing signal or potentially the response of *H. pylori* to that signal.

Preferential accumulation of *H. pylori* relies on chemotaxis signaling and motility. To determine the role of *H. pylori* motility and chemotaxis in damage site colonization, we used *H. pylori* mutants that are nonmotile (Δ*motB*) or nonchemotactic (Δ*cheY*). Following PD, both the Δ*motB* and Δ*cheY* mutants were unable to accumulate at the damage site (Fig. 2A and B). To identify the chemoreceptors involved in the observed accumulation of *H. pylori* at the damage site, we used mutants lacking individual chemoreceptors: the Δ*tlpA*, Δ*tlpB*, Δ*tlpC*, or Δ*tlpD* mutant. During restitution, the *H. pylori* Δ*tlpA*, Δ*tlpC*, and Δ*tlpD* strains accumulated at the damage site by 5 min after PD, whereas the Δ*tlpB* mutant failed to accumulate (Fig. 3A and B). These results demonstrate that chemotaxis signaling and bacterial motility are essential for *H. pylori* accumulation at damage sites, and they suggest that TlpB is the chemoreceptor responsible for the ability of *H. pylori* to sense the damage site.

***H. pylori* accumulation and damage repair.** Since *H. pylori* colonization at damage sites slows repair in the mouse stomach (3), we examined the requirements for chemotaxis and motility in gastroid repair. Previously, we analyzed the repair of the damage area using data fit to a single exponential curve that assumed complete resolution of repair (19, 20). In uninfected gastroids, the closure of the damaged area fit well with an exponential decay curve, resulting in an R^2 value (goodness of fit) of 0.98 ± 0.8 ($n = 8$) (see Fig. S3A and C in the supplemental material). This indicates that the repair of damage was well represented by a single rate constant. However, microinjection of WT *H. pylori* prevented full recovery from damage in gastroids (Fig. 1C), and best-fit curves were observed to consistently underestimate the rate of repair at early time points and to overestimate repair at later time points (Fig. S3B). Under this condition, the single exponential fit had an R^2 value (0.86 ± 0.1) ($n = 5$) significantly lower (Fig. S3C) than that for the bead controls. Therefore, we refined our analyses to examine early and late events separately.

Restricting single exponential fits to the first 6 min of repair, we observed that there was no significant difference in the early repair rate among the control bead, WT *H. pylori*, and mutant *H. pylori* conditions (data not shown). Furthermore, at 3 min following PD, there was no significant difference in the size of the damaged area from the bead control (Fig. 4A), suggesting overall that WT and mutant *H. pylori* strains do not impact early restitution events.

We focused on later repair events by measuring the residual damage area at 16 min following PD, a time point at which damage was consistently sustained in gastroids microinjected with WT *H. pylori*. At 16 min, gastroids microinjected with WT *H. pylori* showed significantly more damage than control gastroids (microinjected with beads)

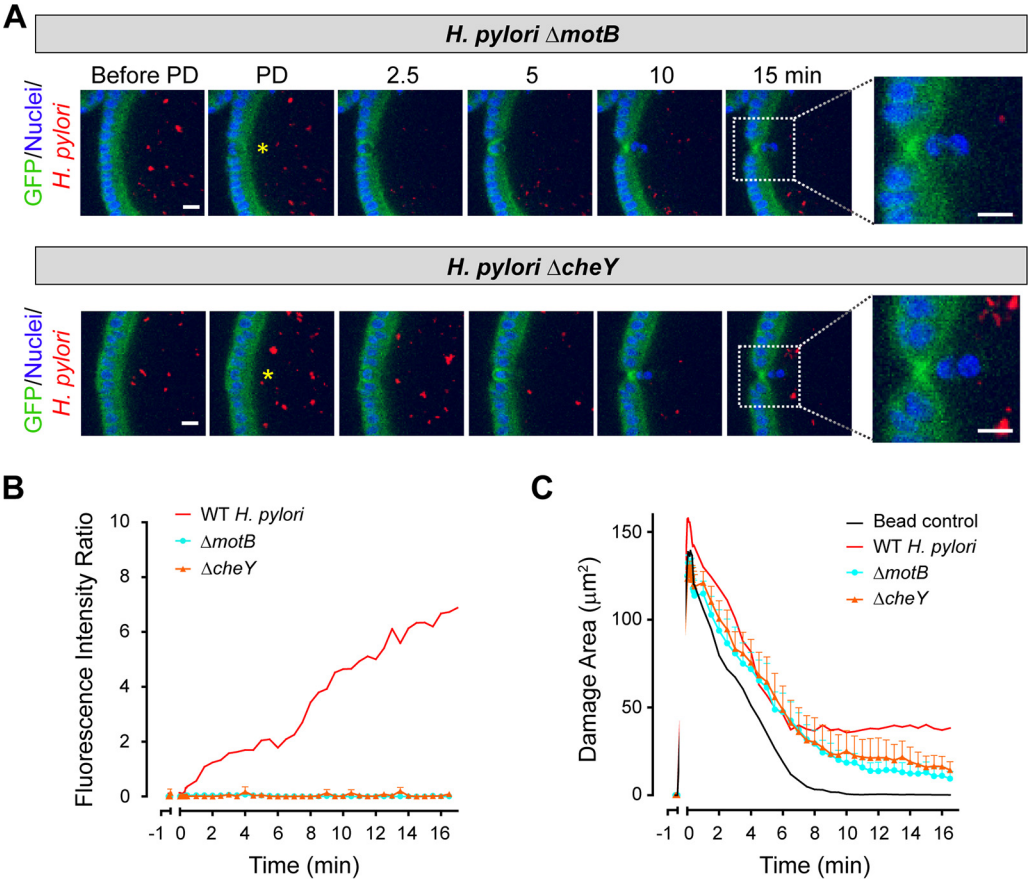

FIG 2 Role of *H. pylori* motility and chemotaxis in *H. pylori* accumulation at the damage site. (A) Representative time course. Shown are confocal images of Hoechst 33342 (10 μg/ml)-stained nuclei (blue), GFP-actin (green), and *H. pylori* Δ*motB* or Δ*cheY* (red). Bars, 10 μm. Yellow asterisks indicate single-cell photodamage (PD) sites. (B) Time course of the fluorescence intensity ratio in gastroids microinjected with the WT (red), Δ*motB* (blue), or Δ*cheY* (orange) *H. pylori* strain. (C) Time course of the damaged area before and following PD in gastroids microinjected with a fluorescent-bead control (black) or the WT (red), Δ*motB* (blue), or Δ*cheY* (orange) *H. pylori* strain. All compiled results are means ± SEM ($n = 6$). In panels B and C, WT *H. pylori* and bead control data were taken from Fig. 1B and C, respectively, for purposes of comparison.

(Fig. 4B). The Δ*tlpA*, Δ*tlpC*, and Δ*tlpD* mutants, which colonized damage sites similarly to WT *H. pylori*, also demonstrated greater residual damage areas (i.e., failure to repair) than the control (Fig. 4B). Gastroids microinjected with an *H. pylori* Δ*motB*, Δ*cheY*, or Δ*tlpB* mutant exhibited smaller damage areas 16 min after PD than those microinjected with WT *H. pylori*, and gastroids microinjected with the Δ*motB* mutant did not differ from those with the bead control (Fig. 4B). These results suggest that *H. pylori* colonization does not delay the early phase of restitution but does inhibit healing events at later times (16 min). Further, only *H. pylori* strains that accumulated at the damage site similarly to the WT (the Δ*tlpA*, Δ*tlpC*, and Δ*tlpD* strains) (Fig. 3C) showed an effect similar to that of the WT in compromising gastric restitution.

Urea in the lumens of gastroids confounds *H. pylori* accumulation. TlpB is the only chemosensor receptor reported to have a high affinity for urea (8). Therefore, to confirm the importance of TlpB independently of the Δ*tlpB* mutant experiments, we added exogenous urea to the lumen. This approach allowed us to test if a high urea concentration in the gastroid lumen would affect *H. pylori* accumulation at the damage site or alter repair. In the presence of 10 mM urea, WT *H. pylori* was unable to accumulate at the damage site (Fig. 5A, B, and D). At 3 min after PD, the damaged areas were similar with the bead control, WT *H. pylori* alone, and WT *H. pylori* in the presence of urea (Fig. 5C and E). However, 16 min after PD in the presence of urea, gastroids

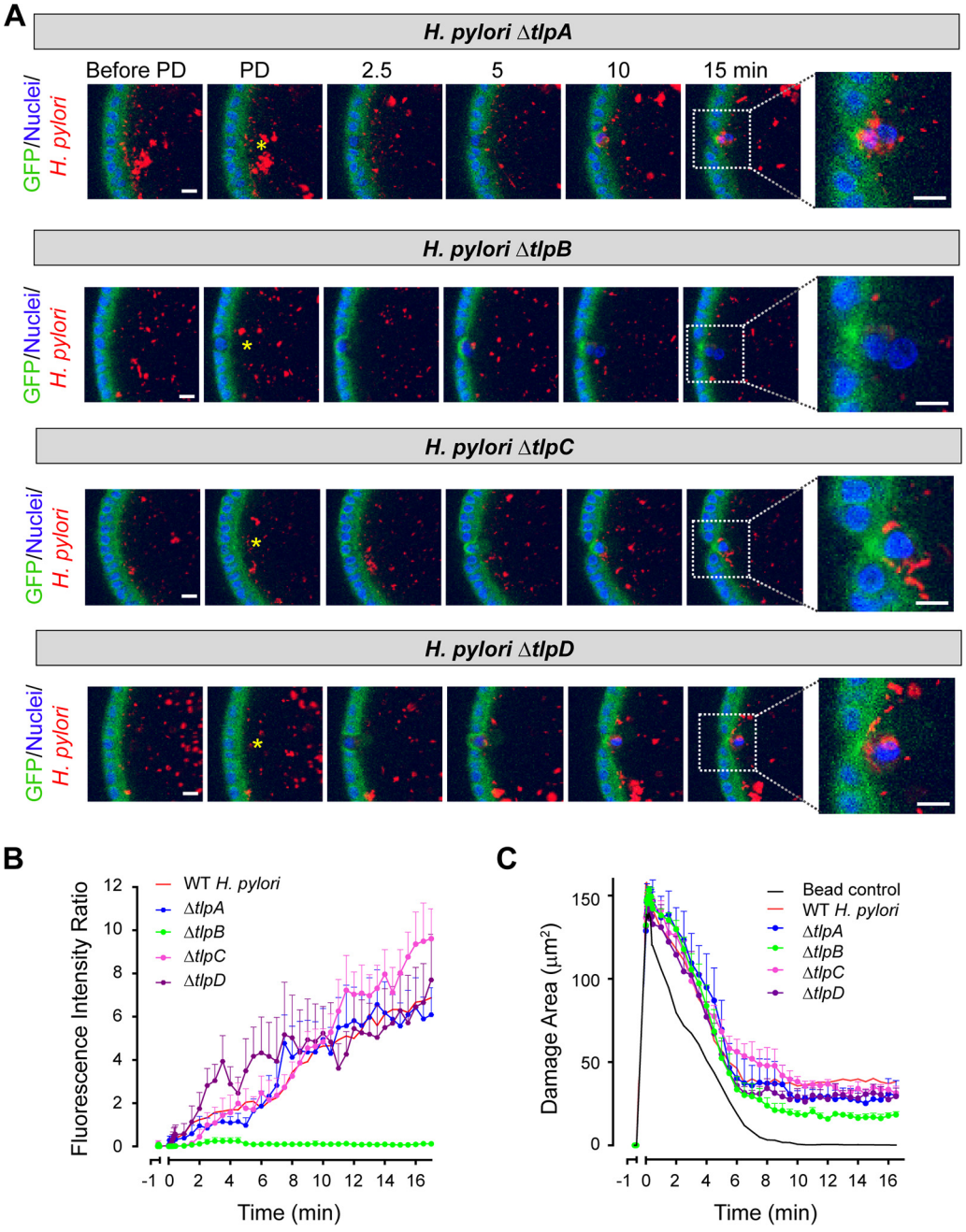

FIG 3 Roles of specific chemoreceptors in *H. pylori* chemotaxis. (A) Representative confocal images of Hoechst 33342 (10 μg/ml)-stained nuclei (blue), GFP-actin (green), and *H. pylori* chemoreceptor mutants (red): the Δ*tlpA*, Δ*tlpB*, Δ*tlpC*, and Δ*tlpD* mutants. Yellow asterisks indicate single-cell photodamage (PD) sites. Bars, 10 μm. (B) Time course of the fluorescence intensity ratio in gastroids microinjected with WT (red), Δ*tlpA* (blue), Δ*tlpB* (green), Δ*tlpC* (pink), or Δ*tlpD* (purple) *H. pylori* strains. (C) Time course of the damaged area before and after PD in gastroids microinjected with fluorescent beads (black) or with WT *H. pylori* (red) or *H. pylori* Δ*tlpA* (blue), Δ*tlpB* (green), Δ*tlpC* (pink), or Δ*tlpD* (purple). Compiled results are means ± SEM for the Δ*tlpA* ($n = 5$), Δ*tlpB* ($n = 6$), Δ*tlpC* ($n = 5$), or Δ*tlpD* ($n = 4$) mutant. In panels B and C, WT *H. pylori* and bead control data were taken from Fig. 1B and C, respectively, for purposes of comparison.

microinjected with WT *H. pylori* exhibited a significantly smaller damaged area than those microinjected with WT *H. pylori* without urea (Fig. 5C and E). In uninfected gastroids, the presence of 10 mM urea did not affect repair (data not shown). These results demonstrate that the presence of urea within the gastroid lumen confounds the ability of *H. pylori* to accumulate at the site of damage, confirming the essential role of TlpB.

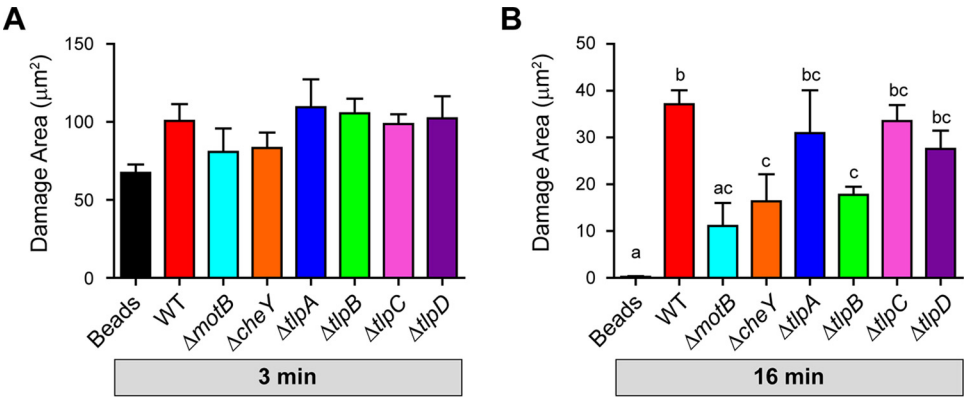

FIG 4 Analysis of the early and later stages of restitution following exposure to *H. pylori*. Results are compiled from Fig. 1 to 3 (bead control and WT *H. pylori* data from Fig. 1C, *H. pylori* Δ*motB* and Δ*cheY* data from Fig. 2C, and chemoreceptor mutant data from Fig. 3C). Shown are measurements of the damage area at 3 min (A) and 16 min (B) after PD in gastroids microinjected with fluorescent beads (black) or the WT (red), Δ*motB* (sky blue), Δ*cheY* (orange), Δ*tlpA* (blue), Δ*tlpB* (green), Δ*tlpC* (pink), or Δ*tlpD* (purple) *H. pylori* strain. All compiled results are means ± SEM. Results represented by bars labeled with the same lowercase letter are not significantly different from each other (a, versus Beads; b, versus WT; c, versus Δ*tlpB*). A *P* level of <0.05 by one-way repeated-measures ANOVA with Dunnett's multiple-comparison test was considered significant.

DISCUSSION

Our study has revealed that gastroids are an excellent model with which to study the impact of *H. pylori* on wound healing and that the *H. pylori* chemoreceptor TlpB is an essential component for sensing sites of gastric injury in this model. We demonstrated previously that *H. pylori* preferentially colonizes injury sites in the stomach via the chemotaxis system in two distinct *in vivo* models (3). In the acetic acid ulceration model, *H. pylori* preferentially colonized the ulcerated area, starting from 1 day postinoculation, which resulted in delayed ulcer healing (3). Additionally, during *in vivo* photodamage (PD) of the gastric epithelium, WT *H. pylori* accumulated at the damage site by 5 min and delayed restitution (3). This study established the general requirement for motility and chemotaxis in order for *H. pylori* to accumulate at the gastric surface and inhibit restitution in these *in vivo* models (3). In agreement with these *in vivo* results, the current *in vitro* study demonstrates that WT *H. pylori* accumulates at damage sites in gastroids, initially accumulating at the damage site ~3 min after PD induction and limiting the repair of damage in the later period up to 16 min following PD. *In vivo*, it is difficult to isolate the host sources necessary for *H. pylori* chemotaxis in response to gastric damage. Potential candidates include molecules generated from blood, subepithelial tissues (lamina propria, endothelial cells, etc.), or epithelial cells. The current work uses primary culture of the gastric epithelium, or gastroids, to demonstrate that chemotactic signals from the epithelium are sufficient to attract *H. pylori* accumulation.

H. pylori utilizes four chemoreceptors, TlpA, TlpB, TlpC, and TlpD, in its chemotaxis system (22, 23). Previous studies have shown that *H. pylori* Δ*tlpB* colonizes normally *in vivo* at early time points (3 to 4 weeks postinfection) when it is the sole infecting *H. pylori* strain (24, 25). However, at later time points (6 weeks postinfection), Δ*tlpB* mutants exhibit lower levels of colonization *in vivo* (25). While these studies have provided insight into the role of TlpB in infection, no study has revealed the chemoreceptor responsible for sensing a gastric injury site. In the present study, only Δ*tlpB* strains were unable to accumulate at the damage site, while *H. pylori* Δ*tlpA*, Δ*tlpC*, and Δ*tlpD* strains accumulated at levels comparable to that of WT *H. pylori* at the damage site. Recently, TlpB was reported to have a high affinity for urea, detecting nanomolar concentrations (8). Our study also shows that experimental addition of luminal urea can confound the ability of WT *H. pylori* to accumulate at the surface. Combined, the results suggest that TlpB is necessary and sufficient as the chemoreceptor responsible for sensing sites of epithelial injury.

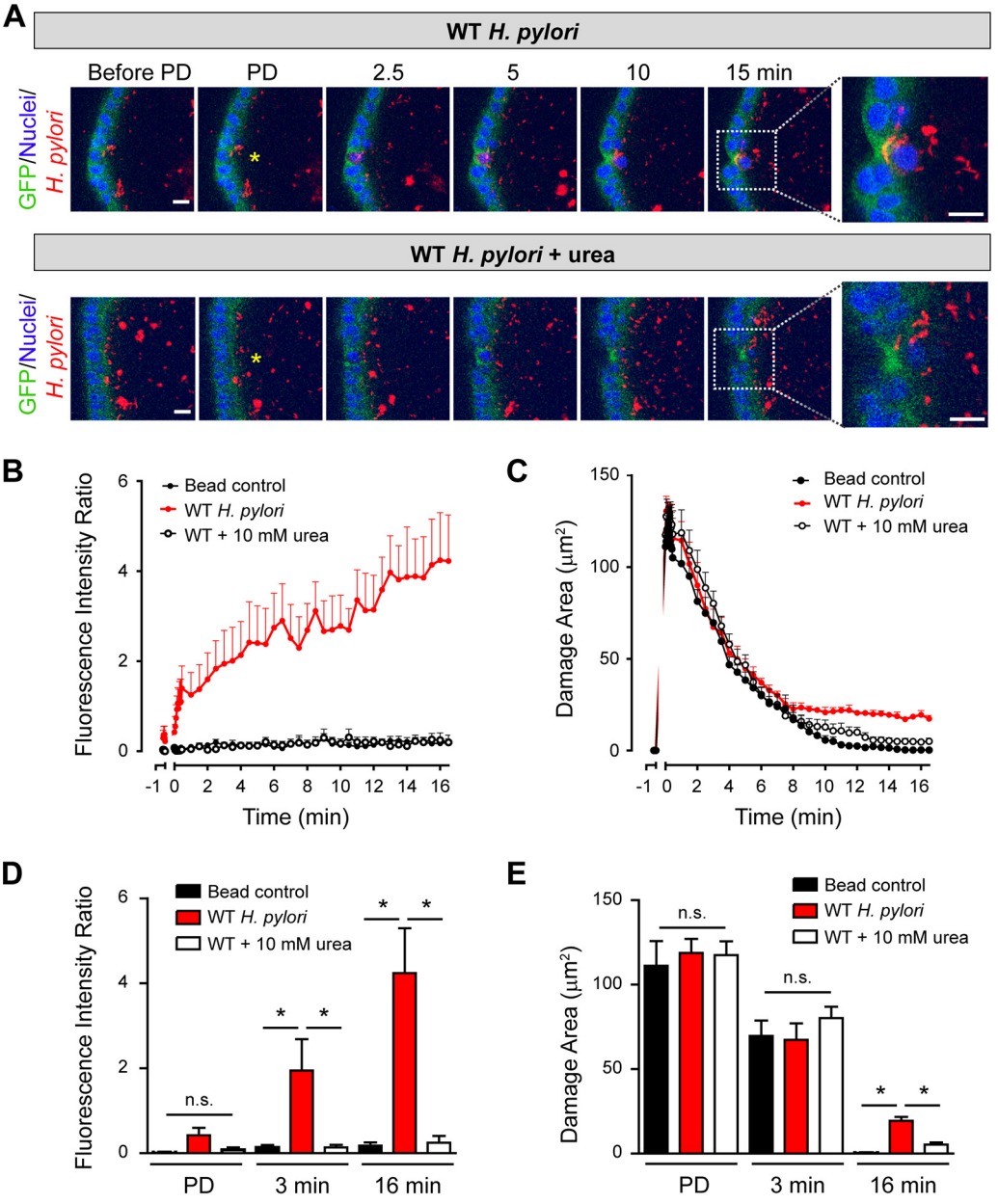

FIG 5 Effects of urea supplementation on *H. pylori* accumulation at damage sites. (A) Representative time course. Shown are confocal images of Hoechst 33342 (10 μg/ml)-stained nuclei (blue), GFP-actin (green), and WT *H. pylori* (red) under control conditions (top) or in the presence of 10 mM urea microinjected into the lumen (bottom). Yellow asterisks indicate single-cell photodamage (PD) sites. Bars, 10 μm. (B and C) Time course of the fluorescence intensity ratio (B) or damage area (C) in gastroids microinjected with a bead control (black), WT *H. pylori* alone (red), or WT *H. pylori* with urea (white). (D and E) Compiled measures of the fluorescence intensity ratio (D) or damage area (E) during PD and at 3 min and 16 min after PD in gastroids microinjected with a bead control (black), WT *H. pylori* alone (red), or WT *H. pylori* with urea (white). Results are means ± SEM for the bead control ($n = 4$), WT *H. pylori* alone ($n = 6$), or WT *H. pylori* in the presence of urea ($n = 7$). Asterisks indicate significance ($P < 0.05$) by one-way repeated-measures ANOVA with Bonferroni's multiple-comparison test. n.s., not significant.

In addition to sensing urea, TlpB has been shown to sense HCl (5) or the quorum-sensing molecule autoinducer 2 (AI-2) (9) as a repellent. It is not clear which molecules participate in the observed chemosensing of damage by TlpB. Not all compounds for *H. pylori* chemoreceptors have been identified, and it is possible that TlpB senses other signals that are present at the sites of injury. Due to the production of circulating urea by the liver and the high membrane permeability of urea, it has been proposed that the gastric mucosa may manifest a concentration gradient of urea moving into the gastric

lumen, which could be the signal for *H. pylori* chemotaxis (26–28). However, it is also possible that the experimental addition of urea masks the ability of *H. pylori* to sense another TlpB attractant. Further studies will be needed to identify the primary signal attracting *H. pylori* colonization.

The inhibition of actin polymerization by Latrunculin A blocks both epithelial repair and *H. pylori* accumulation at the site of damage. These results suggest that the process of epithelial repair (rather than the damage itself) may lead to the generation of the chemotactic signal or, alternatively, that Latrunculin A directly interferes with *H. pylori* function. Supplemental data suggest that bacterial motility is not affected by Latrunculin A, but there may be other, unexpected (and unreported) actions of the drug that directly interfere with bacterial chemosensing. Assuming that the drug acts only on the epithelium, the results would implicate the migrating cells directly neighboring the site of damage, and not the dead cell itself, as the source of the signal(s) sensed by *H. pylori*, since migrating cells have been shown to have altered actin dynamics during epithelial repair (19).

It is not clear why *H. pylori* accumulation slows epithelial repair and why this is evident only after ~6 min of *H. pylori* accumulation. The reason could be simple steric hindrance (bacteria physically getting in the way of the repair process) or potentially a toxic molecule produced by the bacteria. In both cases, the delay in slowing repair could be due to the need to accumulate either bacteria or the toxic product. We speculate that ammonium (NH_4^+) is a candidate secreted toxic factor, since it is produced by *H. pylori* urease as part of the bacterial defense against gastric acid (29, 30) and is known to cause gastric injury and/or to slow restitution (31, 32).

This is the first study to reveal that the *H. pylori* chemoreceptor TlpB plays an important role in *H. pylori* chemotaxis for accumulation at an injury site, and it shows that the host epithelium undergoing repair provides a set of signals sufficient to drive the bacterium to a site of injury. Our results also demonstrate that gastroids provide a suitable model for further exploration of the mechanisms whereby *H. pylori* accumulation at the site of injury delays healing. These findings have the potential to facilitate the development of alternative treatments for *H. pylori*-infected patients, such as targeting TlpB to prevent *H. pylori* sensing and accumulation in areas of gastric injury. This could prove especially useful for patients who do not respond well to the current antibiotic regimen.

MATERIALS AND METHODS

Animal husbandry. The human GFP-actin-expressing (HuGE) heterozygous mice (C57BL/6 background) used in the experiments carried one GFP-actin knock-in allele in the profilin 1 locus (33), and they were confirmed by PCR genotyping. Animals were fed a standard rodent chow diet and had free access to water. Male and female mice were used for experimentation at the age of 2 to 4 months. All animal procedures were approved by the Institutional Animal Care and Use Committee of the University of Cincinnati.

Generation of gastroids. Gastroids from the mouse gastric corpus were generated as described previously (15, 19, 21, 34). Briefly, the isolated mouse gastric corpus was incubated with rocking at 4°C for 2 h in 10 mM EDTA in Dulbecco's phosphate-buffered saline (DPBS) without calcium and magnesium. The tissue was then placed in ice-cold dissociation buffer (43.3 mM sucrose and 54.9 mM D-sorbitol [Sigma], in DPBS) and was shaken forcefully by hand to dissociate individual glands. Dissociated glands were centrifuged at 150 × *g* for 5 min at 4°C, and the pellet was resuspended in Matrigel (Corning). Glands suspended in Matrigel were added to a 2-well Lab-Tek chamber with a cover glass (Thermo Scientific). After Matrigel polymerization at 37°C, advanced Dulbecco's modified Eagle medium (DMEM)/Ham's F-12 supplemented with L-glutamine (2 mM; Thermo Scientific), HEPES (10 mM; Thermo Scientific), penicillin-streptomycin (1×; Corning), N2 and B27 supplements (1×; Life Technologies), Wnt3a conditioned medium (50%), R-Spondin conditioned medium (10%), Noggin conditioned medium (10%), [Leu15]-Gastrin I (10 nM; Sigma), and epidermal growth factor (EGF) (50 ng/ml; PeproTech) was added to the wells and was replaced every 4 days. Gastroids were cultured in a 5% CO_2 incubator at 37°C. For the Latrunculin A (LatA) incubation experiment, LatA (1 μM) was added to the gastroid growth medium 1 h prior to *H. pylori* microinjection. For the urea incubation experiment, the gastroid growth medium was replaced with DMEM/F-12 1 h prior to *H. pylori* microinjection. Urea (10 mM) was added to DMEM/F-12 30 min prior to *H. pylori* microinjection.

Preparation and microinjection of *H. pylori*. For preparation of the *H. pylori* frozen stock, *H. pylori* Sydney strain 1 (WT) and isogenic mutants (the Δ*motB*, Δ*cheY*, Δ*tlpA*, Δ*tlpB*, Δ*tlpC*, and Δ*tlpD* mutants) (14,

25, 35, 36) were grown on Columbia blood agar plates (Remel) containing defibrinated horse blood (5%; Colorado Serum), β-cyclodextrin (0.2%; Sigma), cycloheximide (50 μg/ml; Sigma), vancomycin (5 μg/ml; Sigma), trimethoprim (10 μg/ml; Sigma), and chloramphenicol (for mutants; 5 μg/ml; Sigma) for 3 days. Colonies from these plates tested positive for urease (BD Diagnostic Systems), catalase (using 30% H_2O_2), and oxidase (DrySlide; BD Diagnostic Systems). Bacteria harvested from the plate were grown in Brucella broth (BD Diagnostic Systems) supplemented with 10% heat-inactivated fetal bovine serum (FBS; Fisher Scientific), chloramphenicol (for mutants; 10 μg/ml; Sigma), and a CO_2 gas pack (BD Diagnostic Systems) in a humidified microaerophilic chamber (BBL GasPak system) in an incubator at 37°C overnight. Bacteria were collected and were frozen in Brucella broth (BD Diagnostic Systems) containing 15% glycerol. For experiments, the *H. pylori* frozen stock was used for growing *H. pylori* in Brucella broth (BD Diagnostic Systems) supplemented with 10% FBS in a microaerophilic chamber at 37°C overnight. *H. pylori* was diluted in glycerol, and cells were counted in a hemocytometer. Bacteria were collected by centrifugation at 1,000 × *g* for 5 min and were resuspended in DPBS. To label *H. pylori*, a fluorescent dye (CellTrace Far Red; 1 μM; Invitrogen) was added to DPBS containing *H. pylori* for 20 to 60 min at 37°C. Based on the counting of bacteria, the number of *H. pylori* cells was adjusted to 10^9/ml by resuspension in Brucella broth without serum. As described previously (34), Brucella broth (50 nl) containing 10^6 *H. pylori* bacteria was microinjected into a gastroid by using Nanoject II injectors (Drummond Scientific). Brucella broth (50 nl) containing 10^5 fluorescent beads (diameter, 1.0 μm; Invitrogen) was injected as a control. In some experiments, *H. pylori* was resuspended in Brucella broth (50 nl) containing urea (10 mM) and was used for microinjection.

Induction of two-photon laser-induced microlesions. Experiments were performed in gastroid culture medium under 5% CO_2 at 37°C in a microscope incubation chamber (PeCon, Erbach, Germany) on an inverted confocal microscope (LSM 510 NLO; Zeiss), and the results were imaged with a C-Achroplan NIR 40× objective as described previously (19, 20). Gastroids were preincubated with Hoechst 33342 (10 μg/ml; Thermo Fisher Scientific) for 30 min to visualize cellular nuclei. Images of Hoechst 33342 (Ti-Sa excitation at 730 nm; emission at 435 to 485 nm), GFP-actin (excitation at 488 nm; emission at 500 to 550 nm), fluorescently labeled *H. pylori* (CellTrace: excitation at 633 nm; emission at >650 nm), RFP-tagged *H. pylori* (excitation at 543 nm; emission at >560 nm), and fluorescent beads (excitation at 633 nm; emission at >650 nm) in the gastroid were collected simultaneously with transmitted light. A small rectangular region (≈5 μm^2) of a single cell was repetitively scanned at high Ti-Sa laser power (734 nm; average, 550 mW) for 500 iterations (duration, 2 to 3 s). Gastroids located approximately 150 to 300 μm from the cover glass in the Matrigel were used.

Image analysis. The damaged area was quantified from the time course of images as described elsewhere (19) using ImageJ. The damaged area was measured as the region of cellular loss of GFP fluorescence. The areas that sustained damage were compared at 0, 3, or 16 min after the damage. The fluorescence ratio was calculated from the raw fluorescent intensity of fluorescently labeled *H. pylori* in the area next to the damaged area (10 by 20 μm) divided by the raw fluorescent intensity in the lumen (40 by 70 μm). Outcomes from at least four different gastroids were compiled for each experimental protocol.

Statistical analysis. All values are reported as the means ± standard errors of the means (SEM) from multiple representative experiments. Statistical significance was determined using one-way repeated-measures analysis of variance (ANOVA) with Dunnett's multiple-comparison test or Bonferroni's multiple-comparison *post hoc* test. A P value of <0.05 was considered significant.

SUPPLEMENTAL MATERIAL

Supplemental material for this article may be found at https://doi.org/10.1128/IAI.00202-19.

SUPPLEMENTAL FILE 1, PDF file, 0.1 MB.
SUPPLEMENTAL FILE 2, PDF file, 0.2 MB.
SUPPLEMENTAL FILE 3, MP4 file, 9.4 MB.
SUPPLEMENTAL FILE 4, MP4 file, 5.9 MB.
SUPPLEMENTAL FILE 5, MP4 file, 4.1 MB.
SUPPLEMENTAL FILE 6, MP4 file, 4.3 MB.
SUPPLEMENTAL FILE 7, MP4 file, 4.9 MB.
SUPPLEMENTAL FILE 8, MP4 file, 3.9 MB.

ACKNOWLEDGMENTS

This work was supported by National Institutes of Health (NIH) grant R01DK102551 (to M.H.M. and E.A.) and the Ryuji Ueno Award, cosponsored by the S&R Foundation and the American Physiological Society (to E.A.). H.H. was supported by a "Tobitate! Study abroad scholarship" provided by the Ministry of Education, Culture, Sports, Science and Technology, Japan. This project was also supported in part by NIH grant P30 DK078392 (Live Microscopy Service, Integrative Morphology Core of the Digestive Diseases Research Core Center in Cincinnati).

The funders had no role in study design, data collection and interpretation, or the decision to submit the work for publication.

We thank Chet Closson (University of Cincinnati) for technical assistance with the microscopes. We are very grateful to Walter Witke and Jerrold R. Turner for supplying the HuGE mice. We appreciate Makoto Shimizu, Kazuo Hattori-Kobayashi, and Ken Iwatsuki (Tokyo University of Agriculture, Tokyo, Japan) for supporting the opportunity for H.H. to study abroad.

REFERENCES

1. Marshall BJ, Warren JR. 1984. Unidentified curved bacilli in the stomach of patients with gastritis and peptic ulceration. Lancet i:1311–1315. https://doi.org/10.1016/s0140-6736(84)91816-6.
2. Conteduca V, Sansonno D, Lauletta G, Russi S, Ingravallo G, Dammacco F. 2013. H. pylori infection and gastric cancer: state of the art. Int J Oncol 42:5–18. https://doi.org/10.3892/ijo.2012.1701.
3. Aihara E, Closson C, Matthis AL, Schumacher MA, Engevik AC, Zavros Y, Ottemann KM, Montrose MH. 2014. Motility and chemotaxis mediate the preferential colonization of gastric injury sites by Helicobacter pylori. PLoS Pathog 10:e1004275. https://doi.org/10.1371/journal.ppat.1004275.
4. Schreiber S, Konradt M, Groll C, Scheid P, Hanauer G, Werling H-O, Josenhans C, Suerbaum S. 2004. The spatial orientation of Helicobacter pylori in the gastric mucus. Proc Natl Acad Sci U S A 101:5024–5029. https://doi.org/10.1073/pnas.0308386101.
5. Croxen MA, Sisson G, Melano R, Hoffman PS. 2006. The Helicobacter pylori chemotaxis receptor TlpB (HP0103) is required for pH taxis and for colonization of the gastric mucosa. J Bacteriol 188:2656–2665. https://doi.org/10.1128/JB.188.7.2656-2665.2006.
6. Schweinitzer T, Mizote T, Ishikawa N, Dudnik A, Inatsu S, Schreiber S, Suerbaum S, Aizawa S-I, Josenhans C. 2008. Functional characterization and mutagenesis of the proposed behavioral sensor TlpD of Helicobacter pylori. J Bacteriol 190:3244–3255. https://doi.org/10.1128/JB.01940-07.
7. Cerda OA, Núñez-Villena F, Soto SE, Ugalde JM, López-Solís R, Toledo H. 2011. tlpA gene expression is required for arginine and bicarbonate chemotaxis in Helicobacter pylori. Biol Res 44:277–282. https://doi.org/10.4067/S0716-97602011000300009.
8. Huang JY, Sweeney EG, Sigal M, Zhang HC, Remington SJ, Cantrell MA, Kuo CJ, Guillemin K, Amieva MR. 2015. Chemodetection and destruction of host urea allows Helicobacter pylori to locate the epithelium. Cell Host Microbe 18:147–156. https://doi.org/10.1016/j.chom.2015.07.002.
9. Rader BA, Wreden C, Hicks KG, Sweeney EG, Ottemann KM, Guillemin K. 2011. Helicobacter pylori perceives the quorum-sensing molecule AI-2 as a chemorepellent via the chemoreceptor TlpB. Microbiology 157:2445–2455. https://doi.org/10.1099/mic.0.049353-0.
10. Machuca MA, Johnson KS, Liu YC, Steer DL, Ottemann KM, Roujeinikova A. 2017. Helicobacter pylori chemoreceptor TlpC mediates chemotaxis to lactate. Sci Rep 7:14089. https://doi.org/10.1038/s41598-017-14372-2.
11. Huang JY, Sweeney EG, Guillemin K, Amieva MR. 2017. Multiple acid sensors control Helicobacter pylori colonization of the stomach. PLoS Pathog 13:e1006118. https://doi.org/10.1371/journal.ppat.1006118.
12. Collins KD, Andermann TM, Draper J, Sanders L, Williams SM, Araghi C, Ottemann KM. 2016. The Helicobacter pylori CZB cytoplasmic chemoreceptor TlpD forms an autonomous polar chemotaxis signaling complex that mediates a tactic response to oxidative stress. J Bacteriol 198:1563–1575. https://doi.org/10.1128/JB.00071-16.
13. Howitt MR, Lee JY, Lertsethtakarn P, Vogelmann R, Joubert L-M, Ottemann KM, Amieva MR. 2011. ChePep controls Helicobacter pylori infection of the gastric glands and chemotaxis in the Epsilonproteobacteria. mBio 2:e00098-11. https://doi.org/10.1128/mBio.00098-11.
14. Ottemann KM, Lowenthal AC. 2002. Helicobacter pylori uses motility for initial colonization and to attain robust infection. Infect Immun 70:1984–1990. https://doi.org/10.1128/iai.70.4.1984-1990.2002.
15. Mahe MM, Aihara E, Schumacher MA, Zavros Y, Montrose MH, Helmrath MA, Sato T, Shroyer NF. 2013. Establishment of gastrointestinal epithelial organoids. Curr Protoc Mouse Biol 3:217–240. https://doi.org/10.1002/9780470942390.mo130179.
16. Sato T, Vries RG, Snippert HJ, van de Wetering M, Barker N, Stange DE, van Es JH, Abo A, Kujala P, Peters PJ, Clevers H. 2009. Single Lgr5 stem cells build crypt–villus structures in vitro without a mesenchymal niche. Nature 459:262–265. https://doi.org/10.1038/nature07935.
17. Schumacher MA, Feng R, Aihara E, Engevik AC, Montrose MH, Ottemann KM, Zavros Y. 2015. Helicobacter pylori-induced Sonic Hedgehog expression is regulated by NF-κB pathway activation: the use of a novel in vitro model to study epithelial response to infection. Helicobacter 20:19–28. https://doi.org/10.1111/hel.12152.
18. Wroblewski LE, Piazuelo MB, Chaturvedi R, Schumacher M, Aihara E, Feng R, Noto JM, Delgado A, Israel DA, Zavros Y, Montrose MH, Shroyer N, Correa P, Wilson KT, Peek RM. 2015. Helicobacter pylori targets cancer-associated apical-junctional constituents in gastroids and gastric epithelial cells. Gut 64:720–730. https://doi.org/10.1136/gutjnl-2014-307650.
19. Aihara E, Medina-Candelaria NM, Hanyu H, Matthis AL, Engevik KA, Gurniak CB, Witke W, Turner JR, Zhang T, Montrose MH. 2018. Cell injury triggers actin polymerization to initiate epithelial restitution. J Cell Sci 131:jcs216317. https://doi.org/10.1242/jcs.216317.
20. Engevik KA, Hanyu H, Matthis AL, Zhang T, Frey MR, Oshima Y, Aihara E, Montrose MH. 2019. Trefoil factor 2 activation of CXCR4 requires calcium mobilization to drive epithelial repair in gastric organoids. J Physiol 597:2673–2690. https://doi.org/10.1113/JP277259.
21. Schumacher MA, Aihara E, Feng R, Engevik A, Shroyer NF, Ottemann KM, Worrell RT, Montrose MH, Shivdasani RA, Zavros Y. 2015. The use of murine-derived fundic organoids in studies of gastric physiology. J Physiol 593:1809–1827. https://doi.org/10.1113/jphysiol.2014.283028.
22. Johnson KS, Ottemann KM. 2018. Colonization, localization, and inflammation: the roles of H. pylori chemotaxis in vivo. Curr Opin Microbiol 41:51–57. https://doi.org/10.1016/j.mib.2017.11.019.
23. Keilberg D, Ottemann KM. 2016. How Helicobacter pylori senses, targets and interacts with the gastric epithelium. Environ Microbiol 18:791–806. https://doi.org/10.1111/1462-2920.13222.
24. McGee DJ, Langford ML, Watson EL, Carter JE, Chen Y-T, Ottemann KM. 2005. Colonization and inflammation deficiencies in Mongolian gerbils infected by Helicobacter pylori chemotaxis mutants. Infect Immun 73:1820–1827. https://doi.org/10.1128/IAI.73.3.1820-1827.2005.
25. Williams SM, Chen Y-T, Andermann TM, Carter JE, McGee DJ, Ottemann KM. 2007. Helicobacter pylori chemotaxis modulates inflammation and bacterium–gastric epithelium interactions in infected mice. Infect Immun 75:3747–3757. https://doi.org/10.1128/IAI.00082-07.
26. Yoshiyama H, Nakazawa T. 2000. Unique mechanism of Helicobacter pylori for colonizing the gastric mucus. Microbes Infect 2:55–60. https://doi.org/10.1016/S1286-4579(00)00285-9.
27. Nakamura H, Yoshiyama H, Takeuchi H, Mizote T, Okita K, Nakazawa T. 1998. Urease plays an important role in the chemotactic motility of Helicobacter pylori in a viscous environment. Infect Immun 66:4832–4837.
28. Weng X, Neethirajan S, Vogt A. 2016. Single cell chemotactic responses of Helicobacter pylori to urea in a microfluidic chip. Appl Sci 6:139. https://doi.org/10.3390/app6050139.
29. Hu LT, Mobley H. 1990. Purification and N-terminal analysis of urease from Helicobacter pylori. Infect Immun 58:992–998.
30. Marshall BJ, Barrett LJ, Prakash C, McCallum RW, Guerrant RL. 1990. Urea protects Helicobacter (Campylobacter) pylori from the bactericidal effect of acid. Gastroenterology 99:697–702. https://doi.org/10.1016/0016-5085(90)90957-3.
31. Murakami M, Saita H, Teramura S, Dekigai H, Asagoe K, Kusaka S, Kita T. 1993. Gastric ammonia has a potent ulcerogenic action on the rat stomach. Gastroenterology 105:1710–1715. https://doi.org/10.1016/0016-5085(93)91067-R.

32. Suzuki H, Yanaka A, Muto H. 2000. Luminal ammonia retards restitution of guinea pig injured gastric mucosa in vitro. Am J Physiol Gastrointest Liver Physiol 279:G107–G117. https://doi.org/10.1152/ajpgi.2000.279.1.G107.
33. Gurniak CB, Witke W. 2007. HuGE, a novel GFP-actin-expressing mouse line for studying cytoskeletal dynamics. Eur J Cell Biol 86:3–12. https://doi.org/10.1016/j.ejcb.2006.08.007.
34. Engevik KA, Matthis AL, Montrose MH, Aihara E. 2018. Organoids as a model to study infectious disease. Methods Mol Biol 1734:71–81. https://doi.org/10.1007/978-1-4939-7604-1_8.
35. Andermann TM, Chen Y-T, Ottemann KM. 2002. Two predicted chemoreceptors of Helicobacter pylori promote stomach infection. Infect Immun 70:5877–5881. https://doi.org/10.1128/iai.70.10.5877-5881.2002.
36. Terry K, Williams SM, Connolly L, Ottemann KM. 2005. Chemotaxis plays multiple roles during Helicobacter pylori animal infection. Infect Immun 73:803–811. https://doi.org/10.1128/IAI.73.2.803-811.2005.